Dual-Band BSF with Enhanced Quality Factor

Asmaa E. Farahat and Khalid F. A. Hussein

Microwave Engineering Department
Electronics Research Institute, Cairo, 11843, Egypt
asmaa@eri.sci.eg, khalid_elgabaly@yahoo.com

Abstract ─ In the present work, a U-shaped CPW resonator (CPWR) with, generally, unequal arms is proposed to produce high Q-factor bandstop filter (BSF) based on broadside-coupling between the CPWR and a CPW through-line (CPWTL), which are printed on opposite faces of a thin substrate. The unequal arms of the U-shape and the finite width of the ground strips of the CPWR are shown to produce much higher Q-factor than that of equal arms and infinitely extending side ground planes. The dimensions of the CPWTL are optimized for impedance matching while the dimensions of the CPWR are optimized to obtain the highest Q-factor. The effect of the loss tangent of the dielectric substrate material on the Q-factor is investigated. It is shown that the difference between the lengths of the unequal arms of the U-shaped resonator can be used to control the Q-factor. Thanks to the computational efficiency of the employed electromagnetic simulator, enough number of trials has been successfully performed in reasonable time to arrive at the final design of the BSF. A prototype of the proposed BSF is fabricated for experimental investigation of its performance. The experimental measurements show good agreement when compared with the corresponding simulation results.

Index Terms ─ Bandstop filter, CPW resonator, dual-band filter, high Q-factor.

I. INTRODUCTION

High Q-factor bandpass and bandstop filters can be designed from microwave resonators such as such as printed transmission lines, two and three dimensional cavities such as printed slots and patches. Microwave high Q-factor bandstop filters (BSFs) have been widely used in communication systems for rejecting unwanted frequency signals to enhance the system performance [1-4]. For example, the BSF in the transceiver of the ground station of a satellite communication system. The BSFs are often needed in the frond-end to pass the downlink signals received by the ground station antenna and to block the uplink signals originated at the transmitting antenna of the same ground station. Multiple-band BSFs are required for many applications [5-10].

The principal advantage of CPW is that the signal line and the signal grounds are placed on the same substrate surface. This reduces the dielectric losses and eliminates the need for via holes which simplifies the circuit fabrication. Moreover, the absence of via holes allows simple connection of series as well as shunt components [11-13]. Also, the CPW exhibits lower conductor loss than microstrip lines which is a major advantage [14], [15].

CPW circuits design can be based on both the odd and the even CPW modes [16]. Moreover, CPWs are open structures, and do not require metallic enclosures [17]. Resonators composed of CPW have their distributed element construction avoiding uncontrolled stray inductances and capacitances, and, thereby, have better microwave properties than lumped element resonators.

Q-factor improvement of BSFs has been achieved in literature using printed transmission lines with defected ground structure (DGS) [18-21]. However, the achieved Q-factor is always limited to a few dozens or even lower with some complexity of the structure and needs for lumped elements. The end-coupled and edge-coupled CPW resonator structures are commonly used for microwave and millimeter-wave filter design [22]. The interchange of energy in the end-coupled resonators with the coupling gap may be insufficient, even when very narrow gaps are employed. Due to this reason parallel- or edge-coupled CPWRs are more commonly used than end-coupled CPWRs [22]. However, broadside coupling results in the strongest coupling among all these coupling methods [5]. In [23], a U-shaped CPWR of equal arms has been used to produce high Q-factor BSF. The present work employs U-shaped CPWR of unequal arms to get higher Q-factor. Moreover, the proposed resonator enables more control of the Q-factor by properly setting the difference between the arm lengths of the U-shaped resonator. In the BSF proposed in this work, the CPWR is printed on the bottom layer of the dielectric substrate and the CPW through-line (CPWTL) on the top layer, which enables enhanced broadside coupling. This structure has the advantage that the length over which the broadside coupling is achieved can be easily set to get

the required bandwidth of the BSF or, equivalently, the Q-factor. Another advantage is that the length of the CPWR is simply set to tune the center frequency of the stop band. Moreover, the input impedance of the CPWTL is not sensitive to the substrate thickness, which allows impedance matching independently of the substrate thickness. This provides the design freedom to use the substrate thickness as a major design parameter for controlling the strength of broadside coupling and, hence, the Q-factor of the BSF.

In the following section the proposed design of the BSF is presented. The rules of the design are given in Section III. A prototype of the proposed high Q-factor BSF is fabricated and experimentally studied for more understanding of the underlying physical principles of operation and for verifying some of the simulation results in Section IV.

II. THE PROPOSED BSF DESIGN

The geometry of the BSF proposed in this work is presented in Fig. 1 with the indicated symbolic dimensional parameters. This filter is constructed as a U-shaped CPWR with unequal arms broadside coupled to a CPWTL. Both the CPWR and the CPWTL have finite width ground strips as shown in the figure. The U-shaped CPWR is open-ended half-wavelength resonator. This design necessitates that the strips and slots of the CPWR have the same width as those of the CPWTL. The CPWTL is almost unloaded as long as the operating frequency is far from the resonant frequencies of the U-shaped CPWR, leading to complete microwave power transfer between the filter ports (1) and (2). The microwave power is absorbed and stored in the U-shaped CPWR only over a very narrow frequency band around the resonant frequency, this prevents any power transfer between the filter ports and, thereby, leading to high Q-factor BSF response.

The finite width of the side ground strips of the CPWR results in much higher Q-factor than that obtained when using a CPWR of infinitely extending side ground planes. This is because the lower profile of the CPW with finite-width ground results in lower radiation loss and narrower frequency band for coupling, which, in turn, enhances the Q-factor.

The input impedance (Z_{in}) matching at the filter ports, the center frequency (f_c) and the bandwidth (equivalently the Q-factor), are the most important design goals of the proposed BSF. One of the major advantages of the proposed design is that each of these design goals can be achieved (almost independently of the other two goals) by adjusting only one or two independent parameters. Table 1 gives a list of the dimensional parameters that can be used to achieve the required filter performance metrics.

Each of the design dimensional parameters, (s, w, L_R, L_B, h) can be set to affect significantly one of the

design goal parameters (Z_{in}, f_c, Q) according to Table 1 without significant effects on the other design goal parameters. The theoretical design rules to achieve the BSF design goals are discussed in detail in Section III.
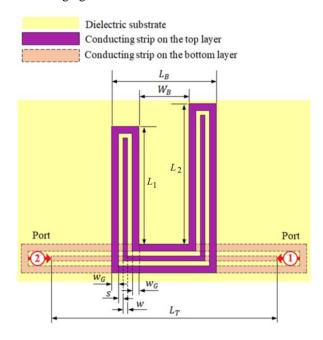

Fig. 1. Schematic of the proposed design for high Q-factor BSF constructed as CPWTL broadside-coupled to a U-Shaped CPWR.

Table 1: List of the independent design parameters that can be used to achieve the design goals of the BSF

Design Goal		Dimensional Parameter	
Symbol	Description	Symbol	Description
Z_{in}	Input Impedance	s	Central Strip Width
		w	Side Slots Width
f_c	Center Frequency	L_R	Resonator Length
Q	Q-Factor	L_B	Coupling Length
		h	Substrate Height

III. THEORETICAL ANALYSIS OF THE BSF DESIGN

The resonance frequency (f_n) of an open-ended CPWR is inversely proportional to the CPWR length (L_R), this can be expressed as follows [17]:

$$f_n = \frac{n\,c}{2L_R\sqrt{\varepsilon_{r_{eff}}}}, \qquad n = 1,2,\dots \qquad (1)$$

where $\varepsilon_{r_{eff}}$ is the effective dielectric constant of the

quasi-TEM mode of the CPW, c is the velocity of light in free space, and n is the resonance mode order.

The effective dielectric constant of the quasi-TEM mode of the CPW can be expressed as follows [17]:

$$\varepsilon_{r_{eff}} = 1 + \frac{\varepsilon_r - 1}{2} \frac{K(\acute{k}_0)}{K(k_0)} \frac{K(k_1)}{K(\acute{k}_1)}, \qquad (2)$$

where ε_r is the dielectric constant of the substrate material and K denotes the complete elliptic integral of the first kind, which is defined as follows:

$$K(k) = \int_0^{\frac{\pi}{2}} \frac{d\theta}{\sqrt{1 - k \sin^2 \theta}}. \qquad (3)$$

The arguments, k_0, $\acute{k}_0$, k_1, and $\acute{k}_1$, of K are defined as follows:

$$k_0 = \frac{s}{s + 2w},$$

$$\acute{k}_0 = \sqrt{1 - k_0^2},$$

$$k_1 = \frac{\sinh\left(\frac{\pi s}{4h}\right)}{\sinh\left[\frac{\pi(s + 2w)}{4h}\right]}, \qquad (4)$$

$$\acute{k}_1 = \sqrt{1 - k_1^2}.$$

The characteristic impedance of the quasi-TEM mode of the CPW is expressed as follows [17]:

$$Z_0 = \frac{30\pi}{\sqrt{\varepsilon_{r_{eff}}}} \frac{K(\acute{k}_0)}{K(k_0)}. \qquad (5)$$

In spite of being formulated for a CPW of infinitely extending ground, the expressions (2) and (5) can be used as preliminary design rules for a CPW with side ground strips of finite width with good accuracy as long as the ground strip width w_G is kept greater than the central strip width and the side slot width. According to (5), by setting the proper values of the strip and slot widths, a 50Ω characteristic impedance of the CPWTL can be obtained.

A. Calculating the Q-factor of the BSF

The resonance frequency of the BSF can be shifted (from that of the unloaded resonator) due to the broadside coupling between the U-shaped CPWR and the CPWTL which causes external loading on the resonator. This is because of reactive coupling, as part of the energy is stored in the electric field of the coupling reactance. The broadside reactive coupling to the through-line can be considered as a loss channel, which decreases the resultant (loaded) Q-factor. Thus, the total (loaded) Q-factor can be evaluated through the following relation.

$$\frac{1}{Q} = \frac{1}{Q_u} + \frac{1}{Q_e}, \qquad (6)$$

where, Q_u is the self or internal (unloaded) Q-factor of the CPWR without being coupled to the through-line and Q_e is the external Q-factor due to coupling. Theoretically, a lossless CPWR has infinite unloaded Q-factor, $Q_u = \infty$. However, practically, Q_u is limited by the conductor and dielectric losses. The external Q-factor Q_e dominates the total Q for low-loss CPWR.

The external Q-factor can be expressed as follows:

$$\frac{1}{Q_e} = \frac{1}{Q_R} + \frac{1}{Q_C}, \qquad (7)$$

where Q_R is an equivalent Q-factor related to the radiation loss and Q_C is an equivalent Q-factor related to the reactive coupling between the resonator and the through-line, which can be considered as a loss channel.

B. Unloaded Q-factor of the CPWR

For the BSF design shown in Fig. 1, the CPW region forming the perimeter of the U-Shape can be considered an open-ended half-wavelength transmission line resonator. The unloaded Q-factor of both short-circuited and open-circuited half-wavelength CPWR can be expressed as follows [17],

$$Q_u = \frac{\pi}{2\alpha L_{R_{1/2}}} = \frac{\beta_0}{2\alpha}\sqrt{\varepsilon_{r_{eff}}} = \frac{\omega_0}{2c\alpha}\sqrt{\varepsilon_{r_{eff}}}, \qquad (8)$$

where, $L_{R_{1/2}}$ is the length of the half-wavelength resonator, β_0 is the free space wave number, ω_0 is the resonant angular frequency, α is the attenuation constant of the CPW, and $\varepsilon_{r_{eff}}$ is given by (2).

The attenuation constant α of the CPW is related by the conductor and dielectric losses and, hence it can be expressed as follows:

$$\alpha = \alpha_c + \alpha_d, \qquad (9)$$

where, α_c is the attenuation caused by the conductor loss whereas α_d is the attenuation caused by the dielectric substrate loss. For a transmission line made of high-conductivity metals like copper ($\sigma = 5.6 \times 10^7 \text{S/m}$) the dielectric loss dominates, which means that $\alpha_d \gg \alpha_c$ and, hence, for a CPW carrying TEM mode, the attenuation constant can be approximated as follows:

$$\alpha \approx \alpha_d = \frac{\omega_0 \tan \delta}{2c}\sqrt{\varepsilon_{r_{eff}}}. \qquad (10)$$

Making use of (10), the expression (8) of the unloaded Q-factor of the CPWR reduces to the following:

$$Q_u \approx \frac{1}{\tan \delta}. \qquad (11)$$

Substituting from (11) into (6), the total Q-factor can be expressed as:

$$Q \approx \frac{Q_e}{1 + Q_e \tan \delta}. \qquad (12)$$

If the loss tangent of the dielectric substrate is known, equation (12) can be used to calculate the external Q-factor, Q_e, given that Q has been obtained by simulation.

C. Calculating the coupling Q-factor using semi-analytical method

It may be useful to assess the effect of the reactive load caused by broadside-coupling to the CPWTL on the Q-factor of the U-shaped CPWR. This can be achieved by evaluating Q_C which is related to reactive coupling. As this Q-factor is difficult to be evaluated analytically, a semi-analytic method it is proposed in the present section. First, the total Q-factor, Q, of the BSF is obtained numerically by electromagnetic simulation, where the commercially available CST™ package is used in the present work for this purpose. A low profile of the CPW ensures low radiation loss and, hence, the term $1/Q_R$ in (7) can be neglected leading to the following expression for the external Q-factor:

$$Q_e \approx Q_C. \tag{13}$$

The last expression means that the external Q-factor is dominated by the coupling Q-factor for well-designed BSF. Making use of (12) and (13), the coupling Q-factor can be evaluated as follows:

$$Q_c \approx \frac{Q}{1 - Q\delta}. \tag{14}$$

IV. NUMERICAL RESULTS AND EXPERIMENTAL MEASUREMENTS

In the present section, both the numerical results obtained by simulation and the experimental results obtained by microwave measurements of the fabricated BSF prototype are presented, discussed and compared for the purpose of arriving at accurate performance assessment and understanding of the resonance mechanism underlying the proposed BSF operation.

In the electromagnetic simulations, for a substrate of size 40 mm × 40 mm and height 0.2 mm, the simulation (execution) time for each of the studied cases to reach the final design is about 20 minutes with accuracy of −40 dB using the frequency domain solver on a core I7-3.6 GHz processor, 16G RAM and 64-bit operating system. Hexahedral meshing is used with 15 cells/wavelength for all simulations.

The results for the external Q-factor obtained by the semi-analytic method described in Section III-C are presented and discussed. It should be noted that the following presentations and discussions of numerical and experimental results are concerned with BSF with unequal arms as that shown in Fig. 1 designed with the following dimensional parameters, unless otherwise stated: $s = 0.1$ mm, $w = 0.1$ mm, $w_G = 0.2$ mm, $L_B = 10$ mm, $W_b = 8.6$ mm, $L_1 = 16.9$ mm, $L_2 = 13.1$ mm, and $L_T = 28$ mm, $L_R = L_1 + L_2 + L_B$. The substrate material is Rogers RO3003C™ with dielectric constant

$\varepsilon_r = 3.38$, dielectric loss tangent $\tan \delta = 0.001$ and height $h = 0.25$ mm. The metal strips and ground are made of copper and have conductivity $\sigma = 5.6 \times 10^7$ S/m. A model with the same dimensions as that of the experimental prototype of the BSF is constructed for electromagnetic simulation using the commercially available CST™ package. This model is presented in Fig. 2 showing the detailed dimensions. At the input and output ports of proposed filter, the transitional tapered CPW region is designed to satisfy impedance matching between the 50Ω impedance of the microwave source and the characteristic impedance of the CPWTL.
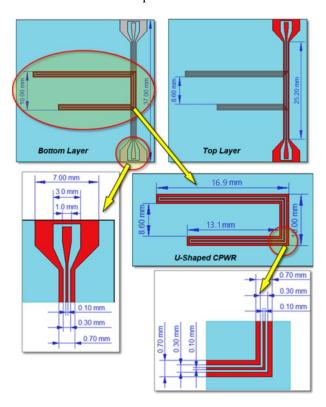

Fig. 2. Dimensions for the CST™ model of the proposed BSF (Note: the red color is for the strips printed on the viewed layer whereas the gray color is for the strips printed on the other layer).

In the following presentation, some comparisons are made between the simulation and experimental results concerned with the frequency response of the BSF at its 1st and 2nd resonances.

A. Frequency response of the proposed BSF

The frequency response of the transmission coefficients $|S_{21}|$ of the proposed dual BSF with the design parameters given in Fig. 2, is presented in Fig. 3. It is assumed that the CPWR is made of copper conductors on a dielectric substrate of $\varepsilon_r = 3$ and loss tangent $\delta = 0.001$. The frequency response exhibits two

sharp anti-peaks: the first one is at $f = 3.12$ GHz , with Q-factor of 155, whereas, the second anti-peak is at $f = 6.25$ GHz, with Q-factor of 46.

The mechanisms leading to these values of the resonant frequencies and the corresponding Q-factors can be explained in view of the surface current distributions at the 1st- and 2nd-order resonance frequencies of the open-ended CPWR formed by the perimeter of the U-shape, which is presented in Fig. 4. At the 1st-order resonance, the current distribution has one maximum value almost centered at the right corner of the U-shape, whereas the current distribution shows two maxima near the centers of the arms of the U-shape.

Fig. 3. Frequency response of the transmission coefficient $|S_{21}|$ of the BSF (with the design shown in Fig. 2) based on the U-shaped half-wave length CPWR.
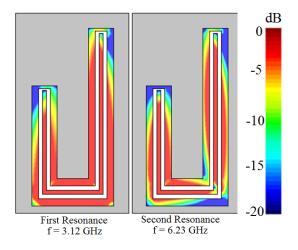

First Resonance
f = 3.12 GHz

Second Resonance
f = 6.23 GHz

Fig. 4. Surface current on the conductors at the frequencies corresponding to the 1st-order and 2nd-order resonances of the U-shaped CPWR.

It is shown that, as this CPW region is a half-wavelength resonator whose total length is 38.4 mm, the resonance frequencies can be calculated using (1), which gives $f_1 = 3.3$ GHz and $f_2 = 6.4$ GHz. The slight deviation of the resonant frequencies obtained by

simulation from the theoretical values obtained by (1) can be attributed to the reactive load resulting from coupling the CPWTL to the CPWR as part of the energy is stored in the electric field of the coupling capacitance and, thereby causing a shift of the resonant frequency. Moreover, a part of the frequency shift can be attributed to the error of the approximate analytic formula for $\varepsilon_{r_{eff}}$ given by (2).

A.1. Tuning the center frequency of the BSF

As given in Table 1, the main design parameter to tune the center frequency of the BSF according to (1) is the total length of the U-shaped CPWR, L_R. Figure 5 shows the change of the frequency response of the transmission coefficient $|S_{21}|$ of the BSF around the 1st resonance frequency with changing the resonator length, L_R while keeping the coupling length L_B constant. It clear that the resonance frequency decreases with increasing the resonator length L_R which agrees with the analytical formula given by (1). This is clear in Fig. 6 (a) which shows that the resonance frequency is inversely proportional to L_R. However, as shown in Fig. 6 (b), the Q-factor is almost independent of the resonator length L_R as long as the coupling length L_B is constant. The effect of the dielectric losses is also shown in Fig. 6 (b), where the increase in the dielectric losses degrades the Q-factor.
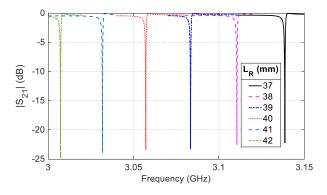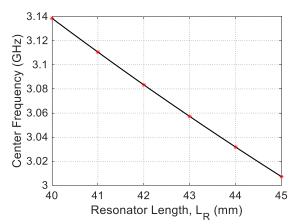

Fig. 5. Change of the frequency response of the transmission coefficient $|S_{21}|$ of the BSF around the 1st resonance frequency with changing the CPWR length, L_R.
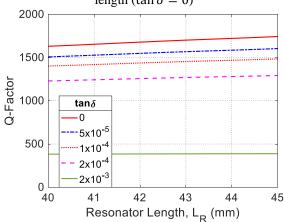
A.2. Adjusting the Q-factor of the BSF

As previously discussed, the Q-factor of the BSF is dominated by the external Q-factor which is attributed mainly to the broadside coupling between the CPWR and the CPWTL. The coupling strength is strongly dependent on the length of the CPW regions over which the coupling is performed. Consequently, the length of the base of the U-shape, L_B, is an important design parameter that controls the Q-factor at each resonance frequency. Figure 7 shows the change of the frequency response of the transmission coefficient $|S_{21}|$ of the BSF

around the 1st resonance frequency with changing the coupling length, L_B, between the CPWR and CPWTL while keeping the total length of the CPWR constant. Figure 8 (a) plots the center frequency with changing L_B. It is clear from Fig. 7 and Fig. 8 (a) that the center frequency is almost constant as long as the resonator length L_R is kept constant. The slight change in the resonance frequency is due to the change of the reactive load impedance as a result of the broadside coupling. The Q-factor is considerably decreased with increasing the coupling length as shown in Fig. 8 (b). As the coupling length increases the reactive load caused by the broadside coupling increases leading to a decrease of the external Q-factor which, in turn, results in considerable decrease of the total Q-factor. The effect of the dielectric losses is investigated in the same figure, it is clear that the increase in $\tan \delta$ decreases the Q-factor.

(a) Dependence of the center frequency on the CPWR length ($\tan \delta = 0$)

(b) Dependence of the Q-factor on the CPWR length for different values of $\tan \delta$

Fig. 6. Dependence of the center frequency and the Q-factor of the BSF on the resonator length at the 1st

resonance frequency of the U-shaped CPWR.

The difference between the two arms of the resonator also affects the Q-factor. In Fig. 9 the frequency response of the transmission coefficient $|S_{21}|$ around the first resonance is studied with changing the difference in the length of the two arms, $d = |L_2 - L_1|$, while keeping the total length of the resonator, L_R constant. The change in the Q-factor with changing the difference d is shown in Fig. 10 at the first and second resonances. It is shown that the best Q-factor is achieved at the second resonance when the difference d is about 7.5 mm.
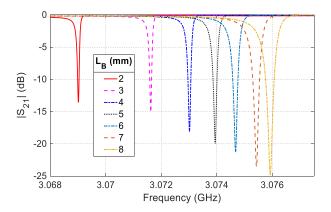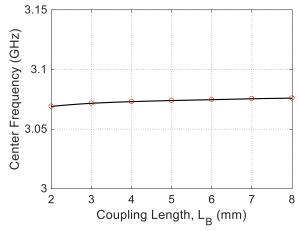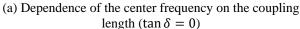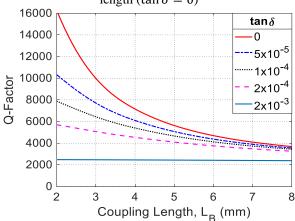

Fig. 7. Change of the frequency response of the transmission coefficient $|S_{21}|$ of the BSF around the 1st resonance frequency with changing the coupling length, L_B, while keeping the CPWR length, L_R constant.

A.3. Effect of substrate height on the Q-factor

The strength of broadside coupling is strongly dependent on the separation distance between the two coupled lines. Consequently, the height of the dielectric substrate, h, is an important design parameter that controls the Q-factor at each resonance frequency. Figure 11 shows the change of the frequency response of the transmission coefficient $|S_{21}|$ of the BSF around the 1st resonance frequency with changing the substrate height. It is clear that the resonance frequency slightly increases with increasing h due to the change of the reactive load impedance equivalent to the broadside coupling. Figure 12 (a) shows that the center frequency is slightly dependent on h. The Q-factor is considerably decreased with increasing the coupling length as shown in Fig. 12 (b). As the substrate height increases the reactive load caused by the broadside coupling increases leading to a decrease of the external Q-factor which, in turn, results in considerable decrease of the total Q-factor. By increasing the dielectric losses, $\tan \delta$, the Q-factor decreases as shown in Fig. 12 (b).

(a) Dependence of the center frequency on the coupling length ($\tan \delta = 0$)

(b) Dependence of the Q-factor on the coupling length for different values of $\tan \delta$

Fig. 8. Dependence of the Q-factor and center frequency of the BSF on the coupling length at the 1st resonance frequency of the U-shaped CPWR.
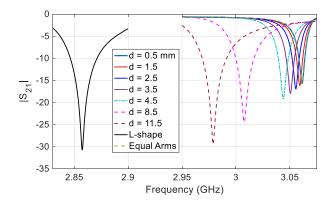

Fig. 9. Change of the frequency response of the transmission coefficient $|S_{21}|$ of the BSF around the 1st resonance frequency with changing the difference, d, between the U-resonator arm lengths.
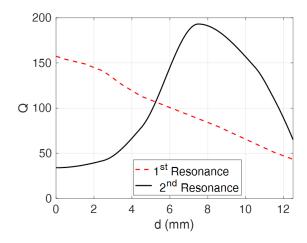

Fig. 10. Dependence of the Q-factor of the BSF at the 1st resonance frequency on the difference, d, between the lengths of the U-shaped CPWR arms.
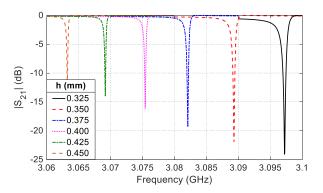

Fig. 11. Change of the frequency response of the transmission coefficient $|S_{21}|$ of the BSF around the 1st resonance frequency with changing the substrate height, h.
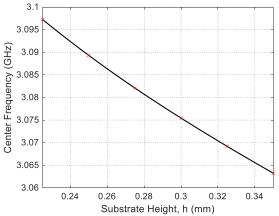
B. Experimental assessment of the BSF

The purpose of the experimental work is to study the underlying physical principles of operation and to investigate the performance of the proposed high Q-factor BSF based on broadside coupling between U-shaped CPWR and CPWTL.
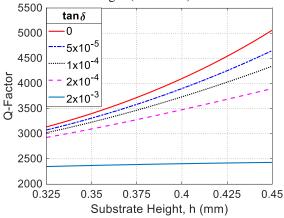
B.1. Prototype fabrication

A prototype of the proposed BSF is fabricated for experimental studying of the underlying physical principles of operation and investigating the filter performance. The dimensional parameters of the fabricated filter are those presented in Fig. 2. The substrate used for fabrication is RO3003C™, with substrate height $h = 0.25$ mm, dielectric constant $\varepsilon_r = 3$ and dielectric loss tangent, $\tan \delta = 0.001$. The same design dimensions given at the beginning of Section IV are used for the fabrication process. A photograph of the fabricated prototypes is presented in Fig. 13, where its size is

compared to a metal coin of the standard one-inch diameter.

(a) Dependence of the center frequency on the substrate height ($\tan\delta = 0$)

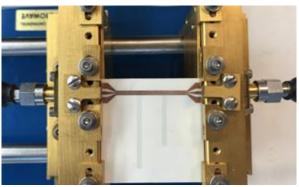(b) Dependence of the Q-factor on the substrate height for different values of $\tan\delta$

Fig. 12. Dependence of the Q-factor and center frequency of the BSF on the substrate height at the 1st resonance frequency of the U-shaped CPWR.

Fig. 13. The fabricated prototype of the proposed high Q-factor BSF.

B.2. Experimental setup

The vector network analyzer (VNA) of the Keysight (Agilent) FieldFox N9928A™ is used to measure the transmission and reflection coefficients $|S_{21}|$ and $|S_{11}|$, respectively, of the BSF prototype under test. For this purpose, the filter prototype is mounted on the substrate test fixture as shown in Fig. 14 (a). After performing the required settings and calibration procedure, the test fixture holding the prototype under test is connected to the VNA as shown in Fig. 14 (b).

(a) The fabricated BSF mounted on the VNA test fixture

(b) Measurement of the transmission coefficient $|S_{21}|$ using the VNA

Fig. 14. Measurement of the frequency response of the fabricated prototype for experimental investigation of the proposed BSF.

B.3. Experimental results

The frequency responses of the transmission and reflection coefficients $|S_{21}|$ and $|S_{11}|$, of this filter over the frequency bands around the 1st resonance is presented in Fig. 15. The measurements are achieved by the VNA and compared to that obtained by simulation using the commercially available CST^{TM} software package. It is clear that the experimental measurements and simulation results show good agreement.

The experimental measurements of the frequency response at the lower band of the BSF show that the 1st resonance occurs at $f_{1st}^{(Exp)} = 3.18$ GHz, whereas and the simulation results show that this resonance occurs at $f_{1st}^{(Sim)} = 3.176$ GHz. The corresponding Q-factors are $Q_{1st}^{(Exp)} = 155$ and $Q_{1st}^{(Sim)} = 168$. The external Q-factor, which is dominated by the coupling Q-factor as discussed before, can be obtained by a semi-analytic approach as described in Section IIIC. The unloaded Q-factor can be calculated in terms of the dielectric substrate loss tangent using (11) to get $Q_u = 457$. The external Q-factor, which is dominantly attributed to broadside coupling, can be obtained by (6) and (12) to get $Q_{e\ 1st}^{(Exp)} = 184$ using the measurement data, and $Q_{e\ 1st}^{(Sim)} = 203$ using the simulation data, where the subscript "1st" indicates the 1st resonance. Such a high value of the external Q-factor can be attributed to the strong broadside coupling between the CPWR and the CPWTL.
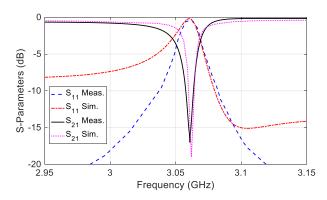

Fig. 15. Frequency responses of the transmission and reflection coefficients $|S_{21}|$ and $|S_{11}|$, respectively, of the BSF at the 1st resonance of the half-wave U-shaped CPWR which is broadside-coupled to the CPWTL.

Comparisons among the Q-factors of some BSFs achieved experimentally in other published work compared with that achieved in the present work are listed in Table 2. The higher value of the Q-factor achieved in the present work is due to the strong broadside coupling and the optimized dimensions of the U-shaped CPWR mainly the coupling length L_c which is the length of the U-shape base.

It should be noted that, the proposed band stop filter design depends on broad side coupling as the feeder is printed on one side of the substrate whereas the resonator is printed on the facing side. This enables much stronger coupling between the feeding and resonator coplanar wave guide regions than that caused by the mechanism used in the other designs such as those presented in Table 2. Moreover, the coupling length (the base of the U-shape) can easily control the coupling strength and hence, the resulting value of the Q-factor.

Table 2: Comparison between Q-factors of BSFs achieved experimentally in other published work compared with that achieved in the present work.

Published Work	Huang et al. [21]	Woo et al. [20]	Liu et al. [2]	Lee et al. [18]	Kakhki et al. [19]	Fahmy et al. [23]	Present Work
Q-Factor	31.7	36.1	45	49.7	57	131	155

V. CONCLUSION

The design of high Q-factor BSF based on broadside-coupling between U-shaped CPWR of unequal arms and CPWTL is presented. The CPWTL is printed on one layer of relatively thin dielectric substrate whereas the CPWR is printed on the opposite layer. The proposed BSF is shown to have much higher Q-factor when compared with other published work. Such high Q-factor is attributed to the unequal arms of the U-shaped CPWR and the finite width of the side ground strips. Due to the lower profile of the CPW with finite-width, the radiation loss is reduced leading to enhanced Q-factor. The dimensions of the CPWTL are optimized for impedance matching whereas the dimensions of the U-shaped CPWR are optimized to obtain the highest possible Q-factor. The numerical results concerned with the effect of the loss tangent of the dielectric substrate material on the Q-factor are presented and discussed. A prototype of the proposed BSF is fabricated and experimentally studied where the measurements show good agreement when compared with the corresponding simulation results.

REFERENCES

[1] Q. Xiang, Q. Feng, and X. Huang, "Tunable BSF based on split ring resonators loaded coplanar waveguide," *Applied Computational Electromagnetics Society Journal*, vol. 28, pp. 591-596, 2013.

[2] G. Liu, Z.-Y. Wang, J.-J. Wu, and L. Li, "Capacitive loaded U-slot defected ground structure for BSF with improvement Q factor," *Progress in Electromagnetics Research*, vol. 65, pp. 31-36, 2017.

[3] H. G. Alrwuili and T. S. Kalkur, "A tunable microstrip BSF using compact spiral folded spurline for RF microwave systems," *International Applied Computational Electromagnetics Society*

Symposium (ACES), 2018.

[4] S. Lee, S. Oh, W.-S. Yoon, and J. Lee, "A CPW BSF using double hairpin-shaped defected ground structures with a high Q factor," *Microwave and Optical Technology Letters*, vol. 58, no. 6, pp. 1265-1268, 2016.

[5] P.-H. Deng, C.-H. Wang, and C. H. Chen, "Novel broadside-coupled bandpass filters using both microstrip and coplanar-waveguide resonators," *IEEE Transactions on Microwave Theory and Techniques*, vol. 54, no. 10, pp. 3746-3750, 2006.

[6] A. Kumar, A. K. Verma, and Q. Zhang, "Compact triple-band BSFs using embedded capacitors," *Progress in Electromagnetics Research*, vol. 63, pp. 15-21, 2016.

[7] S. Yang, Z. Xiao, and S. Budak, "Design of triband BSF using an asymmetrical cross-shaped microstrip resonator," *Progress in Electromagnetics Research*, vol. 86, pp. 35-42, 2019.

[8] J.-M. Yan, L. Cao, and H.-Y. Zhou, "A novel quad-band BSF based on coupled-line and shorted stub-loaded half-wavelength microstrip resonator," *Progress in Electromagnetics Research*, vol. 79, pp 65-70, 2018.

[9] O. A. Safia, A. A. Omar, and M. C. Scardelletti, "Design of dual-band bandstop coplanar waveguide filter using uniplanar series-connected resonators," *Progress in Electromagnetics Research*, vol. 27, pp. 93-99, 2011.

[10] Y. Li, S. Luo, and W. Yu, "A compact tunable triple stop-band filter based on different defected microstrip structures," *Applied Computational Electromagnetics Society*, vol. 33, no. 7, pp. 752-757, 2018.

[11] M. Naser-Moghadasi, "Harmonic suppression of parallel coupled-line bandpass filters using defected microstrip structure," *Applied Computational Electromagnetics Society*, vol. 33, no. 7, pp. 752-757, 2018.

[12] J. K. A. Everard and K. K. M. Cheng, "High performance direct coupled bandpass filters on coplanar waveguide," *IEEE Transactions on Microwave Theory and Techniques*, vol. 41, no. 9, pp. 1568-1573, 1993.

[13] A. Contreras, M. Ribó, L. Pradell, V. Raynal, I. Moreno, M. Combes, and M. Ten, "Compact fully uniplanar BSF based on slow-wave multimodal CPW resonators," *IEEE Microwave and Wireless Components Letters*, vol. 28, no. 9, pp. 780-782, 2018.

[14] K. C. Gupta, R. Garg, and I. Bahl, *Microstrip Lines and Slotlines*. Dedham, MA Artech, 1979.

[15] A. Gopinath, "Losses in coplanar waveguides," *IEEE Transactions on Microwave Theory and Techniques*, vol. 30, no. 7, pp. 1101-1104, 1982.

[16] F. D. Williams and S. E. Schwarz, "Design and performance of coplanar waveguide bandpass filters," *IEEE Transactions on Microwave Theory and Techniques*, vol. 31, no. 7, pp. 558-566, 1983.

[17] R. N. Simons, *Coplanar Waveguide Circuits, Components, and Systems*, vol. 165, John Wiley & Sons, 2004.

[18] S. Lee, S. Oh, W. S. Yoon, and J. Lee, "A CPW BSF using double hairpin-shaped defected ground structures with a high Q factor," *Microwave and Optical Technology Letters*, vol. 58, no. 6, pp. 1265-1268, 2016.

[19] M. A. Kakhki and M. H. Neshati, "Numerical investigation and experimental study of two novel band-reject DGS filters with a very high Q-factor," *19th Iranian Conference on Electrical Engineering, IEEE*, pp. 1-4, 2011.

[20] D. J. Woo, T. K. Lee, J. W. Lee, C. S. Pyo, and W. K. Choi, "Novel U-slot and V-slot DGSs for BSF with improved Q factor," *IEEE Transactions on Microwave Theory and Techniques*, vol. 54, no. 6, pp. 2840-2847, 2006.

[21] S. Y. Huang and Y. H. Lee, "A compact E-shaped patterned ground structure and its applications to tunable bandstop resonator," *IEEE Transactions on Microwave Theory and Techniques*, vol. 57, no. 3, pp. 657-666, 2009.

[22] M. Kumar and R. Gowri, "Review on various issues and design topologies of edge coupled coplanar waveguide filters," *Journal of Graphic Era University*, vol. 5, no. 2, pp. 91-96, 2017.

[23] W. M. Fahmy, A. E. Farahat, K. F. A. Hussein, and A. E. H A. Ammar, "High Q-factor BSF based on CPW resonator broadside-coupled to CPW through-line," *Progress in Electromagnetics Research*, vol. 86, pp. 121-138, 2020.